

## Gravitational Waves from Primordial Black Hole Dark Matter Spikes

WEI-XIANG FENG <sup>1,2</sup> SIMEON BIRD <sup>2</sup> AND HAI-BO YU <sup>2</sup>

<sup>1</sup>*Department of Physics, Tsinghua University, Beijing 100084, China*

<sup>2</sup>*Department of Physics and Astronomy, University of California, Riverside, CA 92521, USA*

### ABSTRACT

The origin of the binary black hole mergers observed by LIGO-Virgo-KAGRA (LVK) remains an open question. We calculate the merger rate from primordial black holes (PBHs) within the density spike around supermassive black holes (SMBHs) at the center of galaxies. We show that the merger rate within the spike is comparable to that within the wider dark matter halo. We also calculate the extreme mass ratio inspiral (EMRI) signal from PBHs hosted within the density spike spiralling into their host SMBHs due to GW emission. We predict that LISA may detect  $\sim 10^4$  of these EMRIs with signal-to-noise ratio of 5 within a 4-year observation run, if all dark matter is made up of PBHs. Uncertainties in our rates come from the uncertain mass fraction of PBHs within the dark matter spike, relative to the host central SMBHs, which defines the parameter space LISA can constrain.

*Keywords:* Gravitational waves (678); Primordial black holes (1292); Supermassive black holes (1663); Dark matter (353)

### 1. INTRODUCTION

**P**RIMORDIAL BLACK HOLES (PBHs) have been proposed as a candidate for dark matter (DM), which makes up 85% of the mass in the Universe (Carr & Hawking 1974; Meszaros 1974; Carr 1975).

Observations from astrophysics and cosmology, notably gravitational microlensing of stars, supernovae and quasars, and accretion effects on the cosmic microwave background, have placed stringent constraints on the PBH DM abundance under the assumption of a monochromatic PBH mass spectrum (see e.g. Carr et al. 2021; Bird et al. 2023). The strongest constraints in the solar mass range are from microlensing surveys of stars in the Large Magellanic Cloud (Allsman et al. 2001; Tisserand et al. 2007; Wyrzykowski et al. 2011; Blaineau et al. 2022).

A new search channel for PBH DM has been opened by the LIGO-Virgo-KAGRA (LVK) detection of gravitational waves (GWs) (Abbott et al. 2023). Indeed, for reasonable PBH DM fractions the predicted merger rate may overlap the  $17.9\text{--}44\text{ Gpc}^{-3}\text{ yr}^{-1}$  range estimated by LVK for binary black hole mergers of mass  $\sim 5\text{--}100 M_{\odot}$  (Bird et al. 2016; Sasaki et al. 2016; Raidal et al. 2017; Ali-Haïmoud et al. 2017; Chen & Huang 2018; Boehm et al. 2021; Hütsi et al. 2021; Franciolini et al. 2022; Jangra et al. 2023).

The rate at which a population of PBHs produces observable GW mergers is uncertain and widely discussed. Bird et al. (2016) suggested that PBH binaries forming via gravitational capture within low redshift halos could match the LVK merger rate if the PBH DM fraction were approximately unity. An alternative channel is the formation of binaries during the radiation-dominated era. Early estimates suggested a larger merger rate and thus implied that a smaller PBH DM fraction ( $f_{\text{PBH}} \sim 10^{-3}$ ) was necessary to match the LVK results (Sasaki et al. 2016; Ali-Haïmoud et al. 2017). However, later analysis suggests that three-body interactions prevent the early binaries thus formed from surviving to the present day (Raidal et al. 2019; Jedamzik 2021, 2020). The LVK merger rate thus still suggests  $f_{\text{PBH}} \sim 1$ , depending on

wxfeng@mail.tsinghua.edu.cn; wfung016@ucr.edu

sbird@ucr.edu

haiboyu@ucr.edu

details of the PBH density distribution, although this is excluded by microlensing surveys.

In this paper, we investigate a novel channel for GW signals: PBHs merging with supermassive black holes (SMBHs) and PBHs forming binaries in the density spike around SMBHs. DM around SMBHs at the center of galaxies will develop a high density region, known as a density spike, within the radius of influence of the SMBH. A DM density spike containing PBHs will have a high PBH density and thus an enhanced LIGO-band merger rate (Nishikawa et al. 2019; Fakhry et al. 2023). This channel can impose even stronger constraints on PBHs than microlensing, as any PBHs in broader DM halos will eventually sink into the galactic center due to mass segregation. Assuming  $f_{\text{PBH}} = 1$  in the spike can still be consistent with microlensing constraints, which enforce  $f_{\text{PBH}} < 1$  in the wider halo.

Extreme mass ratio inspirals (EMRIs) are among the primary sources for the upcoming LISA mission (Gair et al. 2004; Babak et al. 2017; Wang et al. 2020; Bonetti & Sesana 2020; Li et al. 2022; Amaro-Seoane et al. 2023; Colpi et al. 2024). EMRIs could be produced between PBHs in the density spike and the central SMBHs. In this work, we estimate the rate of EMRIs from PBH density spikes and examine the correlation between the EMRI and PBH binary merger rates. The PBH merger rate within the spike is comparable to that within the wider dark matter halo. The dominant EMRI formation channel is not two-body relaxation, as assumed in the literature (Amaro-Seoane et al. 2007; Amaro-Seoane 2018), but GW emission. We show that LISA can place strong constraints on the PBH abundance in the spike.

## 2. MERGER RATE ESTIMATION IN DM SPIKES

Consider two unbound point masses  $m_1$  and  $m_2$  on an initial close encounter with initial relative velocity  $v_{\text{rel}}$ . We assume the orbit is close to parabolic and consider the leading term in the limit eccentricity  $e \rightarrow 1$ . The distance of closest approach is then

$$r_{\text{min}} = \frac{\sigma v_{\text{rel}}^2}{2\pi G(m_1 + m_2)} \quad (1)$$

with  $G$  Newton's constant and  $\sigma$  the scattering cross section. The total energy of gravitational radiation released during the passage is

$$\delta E_{\text{GW}} = \frac{8}{15} \frac{G^{7/2}}{c^5} \frac{(m_1 + m_2)^{1/2} m_1^2 m_2^2}{r_{\text{min}}^{7/2}} g(e) \quad (2)$$

where  $c$  is the speed of light and  $g(e)$  depends only on the eccentricity. The two masses are gravitationally bound and eventually merge if the energy radiated through GW is larger than their initial kinetic energy, i.e.,  $\delta E_{\text{GW}} \gtrsim$

$\frac{1}{2}\mu v_{\text{rel}}^2$ , where  $\mu \equiv \frac{m_1 m_2}{m_1 + m_2}$  is the reduced mass. The merging cross section is then (Quinlan & Shapiro 1989; Mouri & Taniguchi 2002)

$$\sigma_{\text{merg}} = 2\pi \left( \frac{85\pi}{6\sqrt{2}} \right)^{2/7} \frac{G^2(m_1 + m_2)^{10/7} m_1^{2/7} m_2^{2/7}}{c^{10/7} v_{\text{rel}}^{18/7}}, \quad (3)$$

where we have used  $g(e = 1) = 425\pi/32\sqrt{2}$  (Turner 1977). In practice,  $v_{\text{rel}}$  can be approximated by the DM velocity dispersion in a given region.

Consider the following two cases:

- PBH-PBH binary: taking the PBH mass  $m_1 = m_2 = m$ , the merging cross section for two PBHs of equal mass is then

$$\sigma_{\text{merg}}^{\text{PBH}} = 4\pi \left( \frac{85\pi}{3} \right)^{2/7} \frac{G^2 m^2}{c^4} \left( \frac{v_{\text{rel}}}{c} \right)^{-18/7}.$$

- PBH-SMBH inspiral: taking the SMBH mass  $m_1 = M > 10^4 m = 10^4 m_2$  for EMRIs, the merging cross section is then

$$\sigma_{\text{merg}}^{\text{EMRI}} = 2\pi \left( \frac{85\pi}{6\sqrt{2}} \right)^{2/7} \left( \frac{M}{m} \right)^{12/7} \frac{G^2 m^2}{c^4} \left( \frac{v_{\text{rel}}}{c} \right)^{-18/7}.$$

Note that there is a  $(M/m)^{12/7}$  enhancement factor compared to the equal mass merger.

Now we consider  $30 M_{\odot}$  PBHs, which lie in the window  $\sim 20\text{--}100 M_{\odot}$  favored by LVK observations (Carr et al. 2021), and Sgr-A\*-like SMBHs. A central SMBH of mass  $M = 4.3 \times 10^6 M_{\odot}$  (Abuter et al. 2023) has a radius of influence  $r_{\text{sp}} \simeq 2GM/v^2 \simeq 2.2 \text{ pc}$  assuming the stellar velocity dispersion  $v \simeq v_{\text{rel}} \simeq 130 \text{ km/s}$  (as 1D dispersion  $\sigma_* = v/\sqrt{3} \simeq 75 \text{ km/s}$ ). As we will show later, the total mass of  $30 M_{\odot}$  PBH DM residing in the spike  $M_{\text{sp}}$  is (at most) 10% of the SMBH, i.e.,  $0.1M$ . Then the averaged density is  $\rho = 0.1M/V$  within the spike volume  $V = 4\pi r_{\text{sp}}^3/3$ . The merger rate of PBH binaries is

$$\mathcal{R} \simeq (1/2) V (\rho/m)^2 \sigma_{\text{merg}}^{\text{PBH}} v \simeq 1.27 \times 10^{-11} \times \left( \frac{4.3 \times 10^6 M_{\odot}}{M} \right) \left( \frac{v}{130 \text{ km/s}} \right)^{31/7} \text{ yr}^{-1}. \quad (4)$$

The merger rate of EMRIs is

$$\Gamma \simeq (\rho/m) \sigma_{\text{merg}}^{\text{EMRI}} v \simeq 4.55 \times 10^{-7} \left( \frac{4.3 \times 10^6 M_{\odot}}{M} \right)^{2/7} \times \left( \frac{30 M_{\odot}}{m} \right)^{5/7} \left( \frac{v}{130 \text{ km/s}} \right)^{31/7} \text{ yr}^{-1}. \quad (5)$$

Given  $M \propto v^4$  by the  $M\text{--}\sigma_*$  relation (Ferrarese & Merritt 2000; Gebhardt et al. 2000; Tremaine et al. 2002),

Eqs. 4 and 5 imply that  $\mathcal{R} \propto M^{3/28}$  is independent of the PBH mass and *weakly* dependent on the SMBH mass compared to  $\Gamma \propto M^{23/28} m^{-5/7}$ . The EMRI rate is estimated to be four orders of magnitude larger than that of PBH binary mergers in Sgr-A\*-like spikes, and the rate increases with the SMBH mass as  $\Gamma/\mathcal{R} \propto M^{5/7} m^{-5/7}$ . We will show below that the actual enhancement factor is about  $\mathcal{O}(10^2)$ , after taking into account the fact that the distribution of the PBHs is not uniform and their density is higher near the SMBH. In the next section, we provide a more concrete model for the profile of the density spike and calculate the rates more accurately.

### 3. MODELING THE DM DENSITY SPIKE

A DM density spike may develop within the radius of influence  $r_{\text{sp}}$  of a SMBH. Assuming the main halo follows a Navarro-Frenk-White (NFW) profile (Navarro et al. 1996), we consider a density spike following a power-law density profile

$$\rho_{\text{spike}}(r) = \begin{cases} \rho_{\text{sp}} (r/r_{\text{sp}})^{-\alpha}, & 2GM/c^2 < r \leq r_{\text{sp}}; \\ 0, & r \leq 2GM/c^2. \end{cases} \quad (6)$$

Here  $\rho_{\text{sp}}$  is the scale density of the spike, to be fixed, and  $\alpha$  is the logarithmic slope with  $1 \leq \alpha < 3$  depending on astrophysical effects (Ullio et al. 2001; Merritt et al. 2002; Gnedin & Primack 2004). Note that  $\alpha = 1$  corresponds to the NFW inner cusp in the absence of a SMBH and  $\alpha \rightarrow 3$  is the upper limit for a finite spike mass. A single-mass PBH population in the spike which reaches a steady state via gravitational (Coulomb) scattering will follow the Bahcall-Wolf power-law  $\alpha = 7/4$  (Bahcall & Wolf 1976; Alexander 1999; Shapiro & Paschalidis 2014). This is valid only when the spike is fully relaxed. Here we set the lower radial boundary of the spike to be  $2GM/c^2$ . A more detailed calculation gives  $8GM/c^2$  (Gondolo & Silk 1999) (or  $4GM/c^2$  from a general relativistic treatment (Sadeghian et al. 2013; Ferrer et al. 2017)), but this makes a negligible difference to the total spike mass:

$$M_{\text{sp}} = \frac{4\pi\rho_{\text{sp}}r_{\text{sp}}^3}{3-\alpha} \left[ 1 - (2GM/c^2 r_{\text{sp}})^{3-\alpha} \right] \\ \simeq 4\pi\rho_{\text{sp}}r_{\text{sp}}^3/(3-\alpha) \quad (\text{as } r_{\text{sp}} \gg 2GM/c^2). \quad (7)$$

In our numerical study, we will set the spike radius around the SMBH using the Bondi accretion radius,  $r_{\text{sp}} = 2GM/v_{\text{dm}}^2$ , where  $v_{\text{dm}}$  is the velocity dispersion of DM at  $r \gg r_{\text{sp}}$ . For an NFW profile,  $\rho_{\text{NFW}}(r) = \rho_s (r/r_s)^{-1} (1+r/r_s)^{-2}$ , we set  $v_{\text{dm}} = \sqrt{3}\sigma_{\text{dm}} = \sqrt{3GM_{\text{max}}/R_{\text{max}}}$ , where  $\sigma_{\text{dm}}$  is the 1D velocity dispersion of DM and  $M_{\text{max}} = 4\pi\rho_s r_s^3 f(c_{\text{max}})$ , with  $f(x) = \ln(1+x) - x/(1+x)$ , is the mass within

$R_{\text{max}} = c_{\text{max}}r_s = 2.1626r_s$ . As DM halos are in dynamical equilibrium with their central galaxies (Zahid et al. 2018), the DM velocity dispersion  $v_{\text{dm}}$  is approximately the stellar velocity dispersion  $\sqrt{3}\sigma_*$ . The scale density  $\rho_s$  and radius  $r_s$  can be translated into the halo mass  $M_{200}$  and concentration  $c_{200}$ , then we use the  $M$ - $\sigma_*$  relation in Gültekin et al. (2009); Kormendy & Ho (2013) and concentration-mass ( $c_{200}$ - $M_{200}$ ) relation (Prada et al. 2011; Loudas et al. 2022) to associate the central SMBHs to their host halos.

Observationally,  $M_{\text{sp}}$  from DM must be smaller than the uncertainty in determining the dynamical mass  $M$  of the SMBHs, and we set  $M_{\text{sp}} = \Delta M$ . For Centaurus A,  $\Delta \lesssim 0.5$  (Cappellari et al. 2009); Sgr A\*,  $\Delta \lesssim 0.08$  (Gillessen et al. 2009); and M87,  $\Delta \lesssim 0.1$  (Akiyama et al. 2019). A more systematic treatment matches the Bahcall-Wolf spike to the inner cusp of the DM halo profile to fix  $\rho_{\text{sp}}$  with given  $\Delta$ . We choose  $\Delta \simeq 0.1$  to fix  $\rho_{\text{sp}}$  for a SMBH of  $10^9 M_{\odot}$ , which in turn fixes the inner cusp to  $\propto r^{-\gamma}$  with  $\gamma = 1.7$  (see Appendix).

We assume the velocity of PBHs in the spike follows a Maxwell-Boltzmann distribution with a cut-off velocity  $v_{\text{cut}}$ :

$$\mathcal{P}(v, \sigma_{\text{sp}}) = F_0 \left[ \exp\left(-\frac{v^2}{\sigma_{\text{sp}}^2}\right) - \exp\left(-\frac{v_{\text{cut}}^2}{\sigma_{\text{sp}}^2}\right) \right], \quad (8)$$

where  $F_0 = F_0(\sigma_{\text{sp}})$  is the normalization factor and the 1D velocity dispersion of DM in the spike is assumed to be

$$\sigma_{\text{sp}} = \sqrt{\frac{G(M_{\text{sp}} + M)}{r_{\text{sp}}}} = \frac{v_{\text{cut}}}{\sqrt{2}} \quad (9)$$

with the cut-off velocity  $v_{\text{cut}}$  determined by the escape velocity in the density spike. Thus, PBH DM is bound into the spike but might be unbound or loosely bound to the central SMBH, and the velocity-weighted cross section is then  $\langle \sigma_{\text{merg}} v \rangle = \int_0^{v_{\text{cut}}} \mathcal{P}(v, \sigma_{\text{sp}}) \sigma_{\text{merg}} v \, d^3v$ .

### 4. EMRIS V.S. PBH BINARIES

We calculate the rate of PBH mergers within the spike as

$$\mathcal{R} = 4\pi \int_{2GM/c^2}^{r_{\text{sp}}} \frac{1}{2} \left( \frac{\rho_{\text{spike}}(r)}{m} \right)^2 \langle \sigma_{\text{merg}}^{\text{PBH}} v \rangle r^2 \, dr, \quad (10)$$

while the EMRI merger rate is

$$\Gamma = \left( \frac{M_{\text{sp}}/m}{4\pi r_{\text{sp}}^3/3} \right) \langle \sigma_{\text{merg}}^{\text{EMRI}} v \rangle. \quad (11)$$

Both EMRI and PBH mergers depend on central SMBH and halo properties in the same way

$$\left\{ \mathcal{R} \right\} \propto \frac{G^2 \rho_s}{c^3} \frac{M_{200}^2}{M} \frac{D(\sigma_{\text{sp}})}{f^2(c_{200})} \frac{f^3(c_{\text{max}})}{c_{\text{max}}^3}, \quad (12)$$

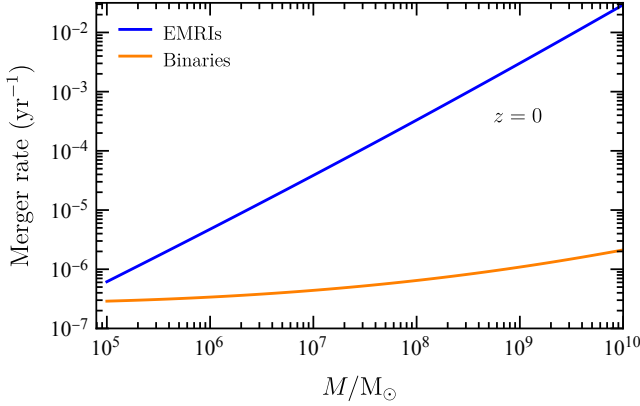


**Figure 1.** Merger rates of EMRI (blue) and PBH binary (orange) per halo as a function of the SMBH mass at redshift  $z = 0$ , assuming the density spike is fully made of PBHs.

up to different enhancement coefficients,  $\mathcal{C}_{\text{PBH}}$  and  $\mathcal{C}_{\text{EMRI}}$ , respectively (see Appendix and Feng (2023) for derivation). Here  $D(\sigma_{\text{sp}})$  is given by

$$D(\sigma_{\text{sp}}) = \int_0^{v_{\text{cut}}} c^3 \mathcal{P}(v, \sigma_{\text{sp}}) \left(\frac{v}{c}\right)^{3/7} d\left(\frac{v}{c}\right) \quad (13)$$

using Eq. 8. As expected,  $\Gamma \propto \mathcal{C}_{\text{EMRI}}/M \sim M^{-2/7} m^{5/7} \Delta$  agrees with Eq. 5. However,  $\mathcal{R} \propto \mathcal{C}_{\text{PBH}}/M \sim [(3-\alpha)^2 \Delta^2 / (2\alpha-3)] (c^2/v_{\text{dm}}^2)^{2\alpha-3} M^{-1}$  differs from Eq. 4 by an extra enhancement  $(c^2/v_{\text{dm}}^2)^{2\alpha-3}$ . This comes from the integration lower bound in Eq. 10 and is due to much higher density near the SMBH. Therefore,  $\Gamma/\mathcal{R} \sim \mathcal{C}_{\text{EMRI}}/\mathcal{C}_{\text{PBH}} \sim [M^{5/7} m^{-5/7} (2\alpha-3)/\Delta(3-\alpha)^2] (v_{\text{dm}}^2/c^2)^{2\alpha-3} \sim \mathcal{O}(10^2)$ , only two orders of magnitude larger, in contrast to our initial estimate. We also note that the merger rates are *sensitive* to the spike fraction  $\Delta$ , where  $\Gamma \propto \Delta$ ; whereas  $\mathcal{R} \propto \Delta^2$ .

Fig. 1 shows the EMRI (blue) and binary (orange) merger rates driven by GW emission. The expected merger rates are comparable  $\mathcal{R} \sim \Gamma \sim 10^{-7} - 10^{-6} \text{ yr}^{-1}$  for SMBHs of  $\sim 10^5 M_{\odot}$ ; while the EMRI merger is more pronounced in higher mass SMBHs, reaching  $\sim 10^{-2} \text{ yr}^{-1}$  at  $\sim 10^{10} M_{\odot}$ , which is four orders of magnitude larger compared to the PBH binary merger. This enhancement is mainly due to the factor  $(M/m)^{5/7}$  with  $M/m > 10^4$ , while the spike fraction  $\Delta$  increases by only an order of magnitude. For Sgr-A\*-like SMBHs, particularly, we find,  $\mathcal{R} \simeq 3.9 \times 10^{-7} \text{ yr}^{-1}$  is comparable to the wider DM halo (Bird et al. 2016; Raidal et al. 2017; Ali-Haïmoud et al. 2017); and  $\Gamma \simeq 1.8 \times 10^{-5} \text{ yr}^{-1}$  is predominant over the estimate of EMRI rates assuming two-body relaxation (Hopman & Alexander 2005, 2006a; Rom et al. 2024).

As discussed previously, the calculation of merger rates shown in Fig. 1 assumes the spike density follows the Bahcall-Wolf profile ( $\alpha = 7/4$ ) (Bahcall & Wolf

1976). This is based on the assumption that the PBHs in the spike are relaxed, and the (two-body) relaxation time should be less than a Hubble time. The relaxation time is  $\sim v^3/G^2 \rho m \ln \Lambda$  (Merritt 2013) with the spike averaged density  $\rho = 3M_{\text{sp}}/4\pi r_{\text{sp}}^3 \gtrsim 3\Delta v^6/32\pi G^3 M^2$  and  $\ln \Lambda \sim \mathcal{O}(10)$  the usual Coulomb logarithm. Using Eq. 8 for root-mean-square velocity  $v_{\text{rms}} \equiv \sqrt{\langle v^2 \rangle}$ , we estimate the relaxation time for the spike as

$$t_{\text{relx}} \simeq \frac{GM^2}{mv_{\text{rms}}^3 \Delta \ln \Lambda} \simeq 9.34 \text{ Gyr} \left(\frac{0.039}{\Delta}\right) \left(\frac{8.3}{\ln \Lambda}\right) \times \left(\frac{M}{4.3 \times 10^6 M_{\odot}}\right)^2 \left(\frac{30 M_{\odot}}{m}\right) \left(\frac{95 \text{ km/s}}{v_{\text{rms}}}\right)^3, \quad (14)$$

which is less than a Hubble time ( $t_H \simeq 14 \text{ Gyr}$ ) only for SMBHs  $\lesssim 10^6 M_{\odot}$ . The relaxation time may be lowered by the presence of stellar objects (other than PBHs) in the spike, with  $\Delta = M_{\text{sp}}/M \sim \mathcal{O}(1)$ . This suggests that spikes could be relaxed in a Hubble time for SMBHs of  $M \lesssim 10^7 M_{\odot}$  (O’Leary et al. 2009; Amaro-Seoane et al. 2023). Larger SMBHs may not have developed the Bahcall-Wolf profile in the spike and may not have a Maxwell-Boltzmann velocity distribution. Although this might alter our predicted merger rates, LISA is likely not sensitive to EMRIs onto SMBHs more massive than  $\sim 10^7 M_{\odot}$ , and so our estimates for SMBHs  $\lesssim 10^7 M_{\odot}$  can still constrain PBHs in the spike.

Note the rates shown in Fig. 1 are conservative as they consider only mergers formed by GW emission. In reality, the SMBHs will be surrounded by nuclear star clusters (Zhou et al. 2024; Mukherjee et al. 2024). PBHs may experience dynamical friction when passing through the stars co-located around SMBHs with the spike. In particular, for relaxed spikes with SMBHs  $\lesssim 10^7 M_{\odot}$ , mass segregation may steepen the spike (to  $\alpha \simeq 2$ ) and enhance the merger rate, as long as the spike mass is dominated by lighter stars (Alexander & Hopman 2009; Preto & Amaro-Seoane 2010; Aharon & Perets 2016). In this case, PBHs may further dissipate their energy and angular momentum by scattering with stars, enhancing merger rates for EMRI and binary formation. Another possible enhancement of the EMRI rate in a relaxed spike is through SMBH binary mergers (Mazzolari et al. 2022; Naoz et al. 2022; Naoz & Haiman 2023). We leave this to future work.

## 5. DIRECT COLLISIONS/PLUNGES AND MERGING TIMESCALES

For mergers to be detectable by LIGO or LISA, they cannot be direct collisions (PBH binaries) or direct plunges (EMRIs). It is thus required that  $r_{\text{min}}$  in Eq. 1 should be larger than the Schwarzschild radius of PBHs or SMBHs. The fraction of PBH-PBH direct colli-



sions scales like  $\propto (v/c)^{4/7}$ , which is less than 1% for  $v \lesssim 240$  km/s. Therefore, direct collisions are negligible. Interestingly, the fraction of PBH-SMBH direct plunges  $\propto (M/m)^{2/7}(v/c)^{4/7}$  is larger than 93% for  $v \gtrsim 240$  km/s and  $M \gtrsim 10^8 M_\odot$ , implying that sufficiently massive SMBHs do not produce EMRIs, but direct plunges. However, once the spin of the SMBH is accounted for, the majority of plunging orbits again become EMRIs (Amaro-Seoane et al. 2013).

We also require that the time for binaries to merge via GW emission is less than the Hubble time, which can be computed from  $r_{\min}$ , the periapsis of the newly formed bound orbits, in Eq. 1 (O’Leary et al. 2009). The characteristic merger time is a function of the average initial separation and thus the PBH velocity dispersion in the spike. For PBH binaries, the merger time ranges from a few days to a few months. For EMRIs, the merger time is much longer,  $10^3$ – $10^4$  years. These timescales are all substantially less than the Hubble time. In addition, it can be easily checked that the PBH number density has to be much higher than that found in the spike for the disruption time to be comparable to their merging time. Three-body effects can thus be ignored for both PBH binaries and EMRIs.

Mergers from two-body relaxation can have a wider range of initial  $r_{\min}$ , and thus their merging times may be much larger than GW-driven mergers. If the merger time is larger than the Hubble time, such binaries would not be detected until GW emission circularizes their orbits. For EMRIs, it has also been shown that only stars or black holes originating from tightly bound orbits with semi-major axes  $\lesssim 10^{-2}$  pc for  $M \sim 10^6 M_\odot$ , can complete their inspiral without being scattered prematurely into the SMBH or onto a wider orbit (Hopman & Alexander 2006b; Merritt et al. 2011).

## 6. EXPECTED EVENTS FROM LIGO AND LISA

To determine the expected LIGO and LISA events, we convolve the merger rates with the SMBH mass function  $dn/d\log M(M)$ . The total merger rate per unit comoving volume is

$$\mathcal{V}_{\{\mathcal{R},\Gamma\}} = \int \frac{dn}{d\log M}(M) \left\{ \begin{array}{l} \mathcal{R}(M) \\ \Gamma(M) \end{array} \right\} d\log M. \quad (15)$$

Fig. 2 shows the convolved EMRI (blue) and PBH binary (orange) merger rates. We adopt two example SMBH mass functions from local Universe measurements for comparison: one using kinematic and photometric data (Shankar et al. 2004) and the other using the spheroid luminosity (Vika et al. 2009). Their differences are moderate. The merger rates of EMRIs and PBH binaries are about the same at  $M \sim 10^5 M_\odot$ ,

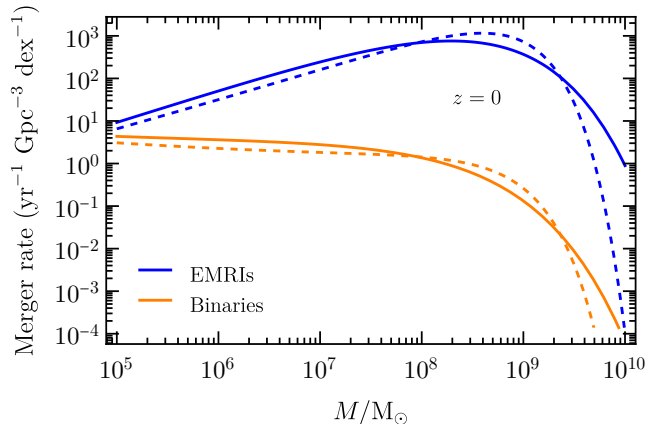


**Figure 2.** EMRI (blue) and PBH binary (orange) merger rates convolved with SMBH mass functions as a function of SMBH mass at redshift  $z = 0$ . The solid lines denote the convolution using kinematic and photometric data based on the empirical relation between the halo velocity dispersion and the SMBH mass (Shankar et al. 2004), while the dashed lines denote the convolution using the spheroid luminosity based on the assumption that all spheroids contain SMBHs at their center (Vika et al. 2009).

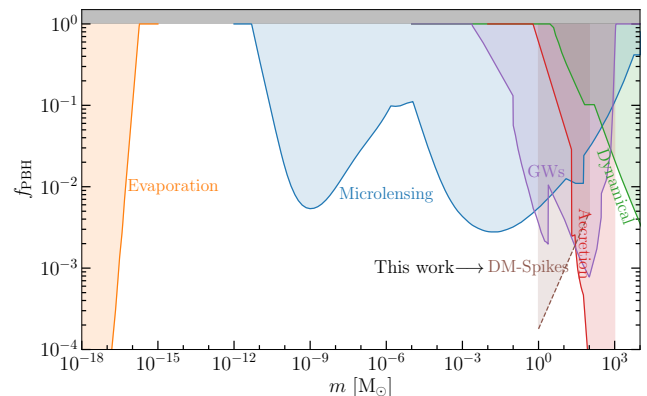


**Figure 3.** PBH fraction  $f_{\text{PBH}}$  in DM as a function of PBH mass  $m$ , assuming a monochromatic mass spectrum. Forecast constraints from EMRIs in DM spikes are given for the mass range  $\sim 1$ – $100 M_\odot$ , assuming that 20 events are detected during LISA’s 4-year observation run with a signal-to-noise ratio of 5. The current constraints for a broader mass range are also shown; from Kavanagh (2019) and the references therein.

however, the EMRI rate increases and reaches a maximum of  $\sim 10^3 \text{ yr}^{-1} \text{ Gpc}^{-3} \text{ dex}^{-1}$  at  $M = 10^8$ – $10^9 M_\odot$ . The average estimated merger rate in the spike is  $\mathcal{V}_{\mathcal{R}} \sim 7 \text{ yr}^{-1} \text{ Gpc}^{-3}$  (PBH binaries); while  $\mathcal{V}_{\Gamma} \sim 1.5 \times 10^3 \text{ yr}^{-1} \text{ Gpc}^{-3}$  (EMRIs).

Generally,  $\mathcal{V}_{\mathcal{R}} \propto f_{\text{PBH}}^2$  while  $\mathcal{V}_{\Gamma} \propto f_{\text{PBH}}$  for GW-driven binary formation. As LIGO and LISA are most sensitive to PBH binaries and EMRIs for  $z \lesssim 1$ , respectively, and the change in the rates is negligible from

$z = 0$  to 1 assuming the same SMBH mass functions, we can ignore redshift evolution. The comoving volume is approximately  $\approx 200 \text{ Gpc}^3$  for  $z \lesssim 1$ , which corresponds to approximately  $\sim 3 \times 10^5$  EMRI events associated with  $\sim 10^3$  PBH binaries per year with  $f_{\text{PBH}} = 1$ ; while we expect  $\sim 3 \times 10^3$  EMRIs associated with  $< 1$  PBH binary per year with  $f_{\text{PBH}} = 0.01$ . However, if a signal-to-noise ratio of 5 is required for EMRI detection (Gair et al. 2004), we obtain a maximal detection redshift of 0.2 and a comoving volume of approximately  $\sim 1.64 \text{ Gpc}^3$ , giving only  $\sim 2500$  events per year.

Fig. 3 shows the forecast constraints on the PBH DM fraction in the mass range  $\sim 1\text{--}100 M_\odot$ , where we assume 20 resolved EMRI events are observed for LISA’s 4-year observation, instead of fixing  $f_{\text{PBH}} = 1$ . This places much stronger constraints than current microlensing surveys:  $f_{\text{PBH}} \sim 10^{-4}\text{--}10^{-3}$ . These constraints are conservative as we assume all the events are from PBHs. In reality, EMRIs could also form when a stellar black hole from a star cluster spirals into a SMBH. If EMRIs could confidently be ascribed to a non-PBH source, then constraints on the PBH abundance in the spike would be stronger.

While unresolved EMRIs will contribute to confusion noise in the stochastic GW background, the merger frequency of these EMRIs are not observable at plausible signal to noise in a midband experiment (Barish et al. 2021) or the nano-Hertz band by Pulsar Timing Array experiments (Agazie et al. 2023; Reardon et al. 2023; Antoniadis et al. 2023; Xu et al. 2023) due to their low GW emissivity at these frequencies. Therefore, LISA remains the most promising facility for constraining PBHs.

## 7. DISCUSSION AND CONCLUSIONS

We have estimated the merger rates in the spike at redshift  $z = 0$  to be  $\mathcal{V}_{\mathcal{R}} \simeq 7 \text{ yr}^{-1} \text{ Gpc}^{-3}$  for PBH binaries, and  $\mathcal{V}_{\Gamma} \simeq 1.5 \times 10^3 \text{ yr}^{-1} \text{ Gpc}^{-3}$  for EMRIs, assuming a PBH DM fraction of  $f_{\text{PBH}} = 1$ . Although we have assumed a single population of PBHs of mass  $\sim 30 M_\odot$ ,

our results should be largely insensitive to a small spread in the mass function around this nominal value. Interestingly, the recent LVK estimation of two merging black holes,  $m_1 \in [5, 50] M_\odot$  and  $m_2 \in [20, 50] M_\odot$  implies an event rate of  $2.5\text{--}6.3 \text{ yr}^{-1} \text{ Gpc}^{-3}$  within the 90% credible range (Abbott et al. 2023). As this is less than our estimates resulting from PBH DM spikes, it suggests  $f_{\text{PBH}} \lesssim 1$  in the spike.

The EMRI mergers arising in the spike could be observed with the future LISA mission (Colpi et al. 2024). As LISA is most sensitive to EMRI systems with mass  $M \simeq 10^4\text{--}10^7 M_\odot$ , the expected EMRI rates for  $M \gtrsim 10^7 M_\odot$  may be below the detection threshold. However, we showed that LISA EMRI rates can place strong constraints on the fraction of DM made up of PBHs. Importantly, the EMRI rate scales as  $f_{\text{PBH}}$ , rather than  $f_{\text{PBH}}^2$  for the binary merger rate, and so retains sensitivity even to low PBH DM fractions. Black hole binary mergers from LVK could also complement this mass range given the correlation  $\Gamma/\mathcal{R} \propto M^{5/7} m^{-5/7}$ . EMRI and PBH merger rates will be spatially correlated, and this correlation may be detectable with more sensitive next-generation ground-based GW experiments, such as the Einstein Telescope (Coccia 2024) and Cosmic Explorer (Reitze et al. 2019), together with space-based GW detectors (DECIGO (Kawamura et al. 2021), LISA, Taiji, and Tianqin (Gong et al. 2021)).

## ACKNOWLEDGEMENTS

WXF acknowledges the support from Anne Kernan Award, Dissertation Year Program Award, and Tsinghua’s Shuimu Scholar Fellow during the completion of this work. This work was supported by NASA ATP 80NSSC22K1897 (SB), the John Templeton Foundation under grant ID#61884 and the U.S. Department of Energy under grant No. DE-SC0008541 (HBY). The opinions expressed in this publication are those of the authors and do not necessarily reflect the views of the funding agencies.

## APPENDIX

### A. SMBH MASS AS A FUNCTION OF HALO MASS

The merger rate generally depends on redshift  $z$  through the scale density and radius of NFW, given by Navarro et al. (1996):

$$\rho_s(z) = \frac{200c_{200}^3 \rho_c(z)}{3f(c_{200})} \quad \text{and} \quad r_s(z) = \left( \frac{3M_{200}}{800\pi c_{200}^3 \rho_c(z)} \right)^{1/3} \quad (\text{A1})$$

with

$$\rho_c(z) = \frac{3H_0^2}{8\pi G} [\Omega_{M,0}(1+z)^3 + \Omega_\Lambda], \quad (\text{A2})$$

$H_0 = 1.02 \times 10^{-4} h \text{ Myr}^{-1}$ ,  $\Omega_{M,0} = 0.315$  and  $\Omega_\Lambda = 0.685$  (Aghanim et al. 2020).

We adopt the  $M\text{--}\sigma_*$  relation (Ferrarese & Merritt 2000; Gebhardt et al. 2000; Tremaine et al. 2002)

$$\log(M/M_\odot) = a_* + b_* \log(\sigma_*/200 \text{ km s}^{-1}) \quad (\text{A3})$$

with the parameters  $a_* = 8.12 \pm 0.08$  and  $b_* = 4.24 \pm 0.41$  (Gultekin et al. 2009; Kormendy & Ho 2013), where we identify

$$\sigma_* = \frac{1}{\sqrt{3}}v_{\text{dm}} = \sqrt{\frac{GM_{\text{max}}}{R_{\text{max}}}} = \sqrt{\frac{4\pi G\rho_s r_s^2 f(c_{\text{max}})}{c_{\text{max}}}}. \quad (\text{A4})$$

To determine the SMBH mass and merger rate, however, we need the concentration-mass ( $c_{200}$ - $M_{200}$ ) relation as a function of redshift (Prada et al. 2011; Ludlow et al. 2014; Correa et al. 2015). We use the following relation (Prada et al. 2011; Loudas et al. 2022):

$$\log c_{200} = 4.23 - 0.25 \log(M_{200}/M_\odot) - 0.16 \log\left(\frac{1+z}{1.47}\right). \quad (\text{A5})$$

In Fig. 4, we plot the SMBH mass as a function of halo mass at redshift  $z = 0$ .

### B. MATCHING THE SPIKE TO THE NFW CUSP

We need to match the spike and NFW profiles. In particular, the total DM spike mass  $M_{\text{sp}}$  and hence  $\Delta$  is sensitive to the inner cusp index  $\gamma$ , which is not necessarily 1, near the spike. We then consider the *modified* NFW profile  $\rho_{\text{NFW}}(r) = \rho_s(r/r_s)^{-\gamma}(1+r/r_s)^{-2} \simeq \rho_s(r/r_s)^{-\gamma}$  when  $r \ll r_s$ , where the cusp index  $\gamma$  ranges from 0 to 2 (Ostriker 2000; de Blok 2010; Shi et al. 2021). In other words, one can determine  $\Delta = \Delta(\alpha, \beta, M, M_{200}, c_{200})$  through matching the modified NFW profile as  $r_{\text{sp}} \ll r_s$ , such that

$$\begin{aligned} \rho_{\text{sp}} &= \rho_{\text{NFW}}(r_{\text{sp}}) = \rho_s(r_{\text{sp}}/r_s)^{-\gamma} \\ &= \rho_s \left( \frac{2M}{3M_{200}} f(c_{200}) \frac{c_{\text{max}}}{f(c_{\text{max}})} \right)^{-\gamma}, \end{aligned} \quad (\text{B6})$$

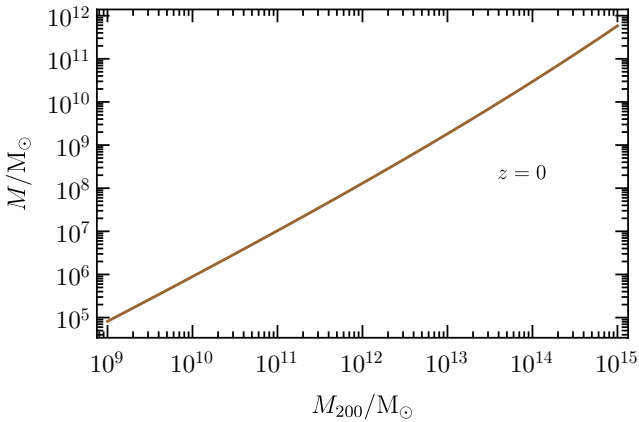


**Figure 4.** SMBH mass as a function of halo mass at redshift  $z = 0$ , following the  $M$ - $\sigma_*$  and concentration-mass relations.

where we have used the Bondi radius as the spike radius<sup>1</sup>

$$\begin{aligned} r_{\text{sp}} &= \frac{2GM}{v_{\text{dm}}^2} = \frac{2M}{3M_{\text{max}}} R_{\text{max}} \\ &= \frac{2M}{3M_{200}} f(c_{200}) \frac{c_{\text{max}}}{f(c_{\text{max}})} r_s. \end{aligned} \quad (\text{B7})$$

Together with the ansatz,  $M_{\text{sp}} = \Delta M \simeq 4\pi\rho_{\text{sp}}r_{\text{sp}}^3/(3-\alpha)$ , we have (see also Feng (2023))

$$\rho_{\text{sp}} = \frac{27}{8}(3-\alpha)\Delta\rho_s \left(\frac{M_{200}}{M}\right)^2 \frac{1}{f^2(c_{200})} \left[\frac{f(c_{\text{max}})}{c_{\text{max}}}\right]^3. \quad (\text{B8})$$

Eqs. B6 and B8 give  $\Delta = \Delta(\alpha, \gamma, M, M_{200}, c_{200})$

$$\begin{aligned} &= \frac{8/27}{3-\alpha} \left(\frac{M}{M_{200}}\right)^2 f^2(c_{200}) \left[\frac{c_{\text{max}}}{f(c_{\text{max}})}\right]^3 \\ &\times \left(\frac{2M}{3M_{200}} f(c_{200}) \frac{c_{\text{max}}}{f(c_{\text{max}})}\right)^{-\gamma}, \end{aligned} \quad (\text{B9})$$

while with the  $M$ - $\sigma_*$  and concentration-mass relations,  $\Delta = \Delta(\alpha, \gamma, M)$  depends only on the black hole mass  $M$ , the spike index  $\alpha$  and the cusp index  $\gamma$ .

Fig. 5 shows the DM spike fraction  $\Delta = M_{\text{sp}}/M$  (top panel), the corresponding Coulomb logarithm  $\ln \Lambda$  (middle panel) and relaxation time to Hubble time ratio  $t_{\text{relx}}/t_H$  (bottom panel). It turns out  $\gamma = 1$  gives  $\Delta \simeq 0.0008$ ;  $\gamma = 1.35$  gives  $\Delta \simeq 0.009$ ;  $\gamma = 1.7$  gives  $\Delta \simeq 0.1$  at  $M = 10^9 M_\odot$  with Bahcall-Wolf spike  $\alpha = 7/4$ .

To compare another definition of  $r_{\text{sp}}$  in the literature, we rewrite

$$M_{\text{sp}} \simeq \frac{4\pi\rho_{\text{sp}}r_{\text{sp}}^3}{3-\alpha} \simeq \frac{4\pi\rho_s (r_{\text{sp}}/r_s)^{-\gamma} r_{\text{sp}}^3}{3-\alpha} = \frac{4\pi\rho_s r_s^\gamma r_{\text{sp}}^{3-\gamma}}{3-\alpha}$$

hence

$$\begin{aligned} r_{\text{sp}} &= \left[ \frac{3-\alpha}{4\pi} \frac{M_{\text{sp}}}{\rho_s r_s^\gamma} \right]^{\frac{1}{3-\gamma}} \\ &= r_s \left[ \frac{3-\alpha}{4\pi} \frac{M_{\text{sp}}}{\rho_s r_s^3} \right]^{\frac{1}{3-\gamma}} = r_s \left[ \frac{3-\alpha}{4\pi} \frac{\Delta M}{\rho_s r_s^3} \right]^{\frac{1}{3-\gamma}}. \end{aligned} \quad (\text{B10})$$

In the literature (Merritt 2003; Lenoci 2023), a commonly used definition for  $r_{\text{sp}}$  is through the enclosed mass of dark matter within the “radius of influence”  $r_h$  equals to two times the central SMBH mass, i.e.,

<sup>1</sup> Technically, the Bondi radius  $r_B = 2GM/c_s^2$  is defined through the “sound speed”  $c_s$  of the accreted gas far away from the Bondi radius (Armitage 2020). For PBHs as DM, the “effective”  $c_s^2 = (5/9)v_{\text{dm}}^2$ , thus the spike radius  $r_{\text{sp}} = 2GM/v_{\text{dm}}^2$  is smaller than  $r_B$ .

$M_{\text{dm}}(r < r_h) = 2M$  and the spike extends up to  $r_{\text{sp}} \simeq 0.2r_h$ . This implies

$$2M = \frac{4\pi\rho_{\text{sp}}(r_{\text{sp}}/0.2)^{3-\alpha}}{3-\alpha} r_{\text{sp}}^\alpha$$

thus

$$r_{\text{sp}} = \left[ \frac{(0.2)^{3-\alpha}(3-\alpha)M}{2\pi\rho_{\text{sp}}} \right]^{1/3} = \left[ \frac{(0.2)^{3-\alpha}(3-\alpha)M}{2\pi\rho_s(r_{\text{sp}}/r_s)^{-\gamma}} \right]^{1/3}$$

Solving for  $r_{\text{sp}}$ , we obtain

$$r_{\text{sp}} = r_s \left[ \frac{(0.2)^{3-\alpha}(3-\alpha)M}{2\pi\rho_s r_s^3} \right]^{\frac{1}{3-\gamma}}. \quad (\text{B11})$$

In comparison, this definition *automatically* fixes the spike fraction to be  $\Delta = \Delta(\alpha) = 2 \times (0.2)^{3-\alpha} = 0.267$  for spike index  $\alpha = 1.75$ , independent of the halo properties and the black hole mass.

### C. MERGER RATES DRIVEN BY GW EMISSION

The velocity-weighted cross sections for PBH mergers and EMRIs are

$$\langle \sigma_{\text{merg}}^{\text{PBH}} v \rangle = (4\pi)^2 \left( \frac{85\pi}{3} \right)^{2/7} \frac{G^2 m^2}{c^3} D(\sigma_{\text{sp}}) \quad (\text{C12})$$

and

$$\langle \sigma_{\text{merg}}^{\text{EMRI}} v \rangle = (4\pi)^2 \left( \frac{85\pi}{96} \right)^{2/7} \left( \frac{M}{m} \right)^{12/7} \frac{G^2 m^2}{c^3} D(\sigma_{\text{sp}}), \quad (\text{C13})$$

respectively, where

$$D(\sigma_{\text{sp}}) = \int_0^{v_{\text{cut}}} c^3 \mathcal{P}(v, \sigma_{\text{sp}}) \left( \frac{v}{c} \right)^{3/7} d \left( \frac{v}{c} \right). \quad (\text{C14})$$

Then the resulting merger rates for PBH binaries and EMRIs are

$$\begin{aligned} \left\{ \begin{array}{l} \mathcal{R} \\ \Gamma \end{array} \right\} &= \left\{ \begin{array}{l} \mathcal{C}_{\text{PBH}} \\ \mathcal{C}_{\text{EMRI}} \end{array} \right\} \frac{G^2 \rho_s M}{c^3} \left( \frac{M_{200}}{M} \right)^2 \\ &\times \frac{D(\sigma_{\text{sp}})}{f^2(c_{200})} \left[ \frac{f(c_{\text{max}})}{c_{\text{max}}} \right]^3 \end{aligned} \quad (\text{C15})$$

with

$$\begin{aligned} \mathcal{C}_{\text{PBH}} &= 27\pi^2 \left( \frac{85\pi}{3} \right)^{2/7} (3-\alpha)^2 \Delta^2 \\ &\times \begin{cases} \left( \frac{1}{3-2\alpha} \right) \left[ 1 - (v_{\text{dm}}^2/c^2)^{3-2\alpha} \right] & (\alpha \neq 3/2) \\ \ln(c^2/v_{\text{dm}}^2) & (\alpha = 3/2) \end{cases} \end{aligned} \quad (\text{C16})$$

and

$$\mathcal{C}_{\text{EMRI}} = 162\pi^2 \left( \frac{85\pi}{96} \right)^{2/7} \left( \frac{M}{m} \right)^{5/7} \Delta, \quad (\text{C17})$$

respectively. We set  $v_{\text{dm}}^2 = 3GM_{\text{max}}/R_{\text{max}} = 12\pi G\rho_s r_s^2 f(c_{\text{max}})/c_{\text{max}}$  to associate with the halo properties.

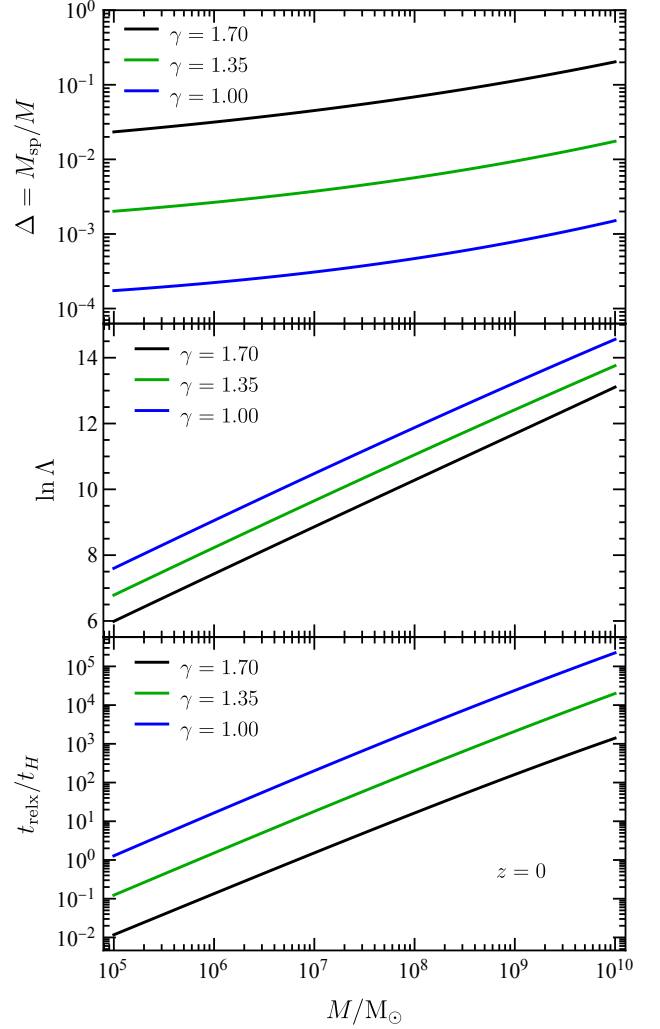


**Figure 5.** The ratio of spike to SMBH masses (top panel), Coulomb logarithm (middle panel), ratio of relaxation time to the Hubble time (bottom panel) at redshift  $z = 0$ , following the  $M$ - $\sigma_*$  and concentration-mass relations. We assume Bahcall-Wolf power-law  $\alpha = 7/4$  for inner cusp indices  $\gamma = 1.7, 1.35, \text{ and } 1$ . The PBH mass is  $30 M_\odot$ .

### D. THE SMBH MASS FUNCTIONS AND MERGER RATES

We consider two SMBH mass functions. First, the estimated SMBH mass function according to kinematic and photometric data based on the empirical relation between the halo velocity dispersion and the SMBH mass in Shankar et al. (2004),

$$\frac{dn}{d \log M}(M) = \phi_* \left( \frac{M}{M_*} \right)^{A+1} \exp \left[ - \left( \frac{M}{M_*} \right)^B \right] \quad (\text{D18})$$

with  $\phi_* = 7.7 \times 10^6 \text{ Gpc}^{-3}$ ,  $M_* = 6.4 \times 10^7 M_\odot$ ,  $A = -1.11$  and  $B = 0.49$ . The other one is based on the assumption that all spheroids contain SMBHs at their



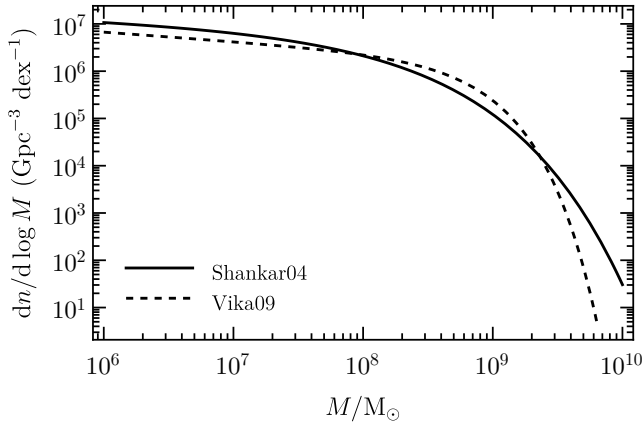


**Figure 6.** Estimated SMBH mass functions using kinematic and photometric data based on the empirical relation between the halo velocity dispersion and the SMBH mass in Shankar et al. (2004), and using the spheroid luminosity based on the assumption that all spheroids contain SMBHs at their center in Vika et al. (2009).

PBH binary merger rates ( $\text{yr}^{-1} \text{Gpc}^{-3}$ )		
Inner cusp index $\gamma$	Shankar04	Vika09
1.70	$8.00776 \times 10^0$	$5.88495 \times 10^0$
1.35	$5.73483 \times 10^{-2}$	$4.21906 \times 10^{-2}$
1.00	$3.99449 \times 10^{-4}$	$2.93342 \times 10^{-4}$
EMRI merger rates ( $\text{yr}^{-1} \text{Gpc}^{-3}$ )		
Inner cusp index $\gamma$	Shankar04	Vika09
1.70	$1.36129 \times 10^3$	$1.61796 \times 10^3$
1.35	$1.18750 \times 10^2$	$1.41930 \times 10^2$
1.00	$9.88148 \times 10^0$	$1.18237 \times 10^1$

**Table 1.** The merger rates of  $30 M_{\odot}$  PBH binaries and EMRIs with various inner cusp indices  $\gamma = 1.7, 1.35,$  and  $1$  to match the DM spike of Bahcall-Wolf power-law  $\alpha = 7/4$ , given the SMBH functions in Shankar et al. (2004) and Vika et al. (2009).

center, using 1743 galaxies from the Millennium Galaxy Catalogue in Vika et al. (2009),

$$\frac{dn}{d \log M}(M) = \phi_* \left(\frac{M}{M_*}\right)^{A+1} \exp \left[1 - \left(\frac{M}{M_*}\right)\right] \quad (\text{D19})$$

with  $\phi_* = 7.07946 \times 10^5 \text{Gpc}^{-3}$ ,  $M_* = 10^{8.71} M_{\odot}$  and  $A = -1.2$ . See Fig. 6 for comparison of the two mass functions and Table 1 for the corresponding PBH binary and EMRI merger rates of  $30 M_{\odot}$  PBHs with inner cusp indices  $\gamma = 1.7, 1.35,$  and  $1$ .

In the main text, we assume  $\Delta \simeq 0.1$  (of all PBH DM) at  $M = 10^9 M_{\odot}$  but vary with the SMBH mass, which fixes inner cusp index of all halos to be  $\gamma = 1.7$ . Assuming  $\Delta = 0.1$  uniformly over the whole SMBH spectrum will result in more enhancement of  $\mathcal{V}_{\mathcal{R}} \sim 35\text{--}53 \text{yr}^{-1} \text{Gpc}^{-3}$  (PBH binaries), while  $\mathcal{V}_{\Gamma} \sim 2 \times 10^3 \text{yr}^{-1} \text{Gpc}^{-3}$  (EMRIs), from GW-driven processes. Moreover, if we adopt the spike radius  $r_{\text{sp}}$  by setting the enclosed DM mass  $M_{\text{dm}}(r < r_{\text{sp}}/0.2) = 2M$  (Merritt 2003; Lenoci 2023), the DM fraction  $\Delta = 0.267$  is fixed and much more events are expected. In this regard, our estimated rates shown in the main text are conservative.

## REFERENCES

- Abbott, R., et al. 2023, Phys. Rev. X, 13, 011048, doi: [10.1103/PhysRevX.13.011048](https://doi.org/10.1103/PhysRevX.13.011048)
- Abuter, R., et al. 2023, Astron. Astrophys., 677, L10, doi: [10.1051/0004-6361/202347416](https://doi.org/10.1051/0004-6361/202347416)
- Agazie, G., et al. 2023, Astrophys. J. Lett., 951, L8, doi: [10.3847/2041-8213/acdac6](https://doi.org/10.3847/2041-8213/acdac6)
- Aghanim, N., et al. 2020, Astron. Astrophys., 641, A6, doi: [10.1051/0004-6361/201833910](https://doi.org/10.1051/0004-6361/201833910)
- Aharon, D., & Perets, H. B. 2016, Astrophys. J. Lett., 830, L1, doi: <https://doi.org/10.3847/2041-8205/830/1/L1>
- Akiyama, K., et al. 2019, Astrophys. J. Lett., 875, L6, doi: [10.3847/2041-8213/ab1141](https://doi.org/10.3847/2041-8213/ab1141)
- Alexander, T. 1999, Astrophys. J., 527, 835, doi: [10.1086/308129](https://doi.org/10.1086/308129)
- Alexander, T., & Hopman, C. 2009, Astrophys. J., 697, 1861, doi: [10.1088/0004-637X/697/2/1861](https://doi.org/10.1088/0004-637X/697/2/1861)
- Ali-Haïmoud, Y., Kovetz, E. D., & Kamionkowski, M. 2017, Phys. Rev. D, 96, 123523, doi: [10.1103/PhysRevD.96.123523](https://doi.org/10.1103/PhysRevD.96.123523)
- Allsman, R. A., et al. 2001, Astrophys. J. Lett., 550, L169, doi: [10.1086/319636](https://doi.org/10.1086/319636)
- Amaro-Seoane, P. 2018, Living Rev. Rel., 21, 4, doi: [10.1007/s41114-018-0013-8](https://doi.org/10.1007/s41114-018-0013-8)

- Amaro-Seoane, P., Gair, J. R., Freitag, M., et al. 2007, *Class. Quant. Grav.*, 24, R113, doi: [10.1088/0264-9381/24/17/R01](https://doi.org/10.1088/0264-9381/24/17/R01)
- Amaro-Seoane, P., Sopuerta, C. F., & Freitag, M. D. 2013, *Mon. Not. Roy. Astron. Soc.*, 429, 3155, doi: [10.1093/mnras/sts572](https://doi.org/10.1093/mnras/sts572)
- Amaro-Seoane, P., et al. 2023, *Living Rev. Rel.*, 26, 2, doi: [10.1007/s41114-022-00041-y](https://doi.org/10.1007/s41114-022-00041-y)
- Antoniadis, J., et al. 2023, *Astron. Astrophys.*, 678, A50, doi: [10.1051/0004-6361/202346844](https://doi.org/10.1051/0004-6361/202346844)
- Armitage, P. J. 2020, *Astron. Geophys.*, 61, 2.40, doi: [10.1093/astrogeo/ataa032](https://doi.org/10.1093/astrogeo/ataa032)
- Babak, S., Gair, J., Sesana, A., et al. 2017, *Phys. Rev. D*, 95, 103012, doi: [10.1103/PhysRevD.95.103012](https://doi.org/10.1103/PhysRevD.95.103012)
- Bahcall, J. N., & Wolf, R. A. 1976, *Astrophys. J.*, 209, 214, doi: [10.1086/154711](https://doi.org/10.1086/154711)
- Barish, B. C., Bird, S., & Cui, Y. 2021, *Phys. Rev. D*, 103, 123541, doi: [10.1103/PhysRevD.103.123541](https://doi.org/10.1103/PhysRevD.103.123541)
- Bird, S., Cholis, I., Muñoz, J. B., et al. 2016, *Phys. Rev. Lett.*, 116, 201301, doi: [10.1103/PhysRevLett.116.201301](https://doi.org/10.1103/PhysRevLett.116.201301)
- Bird, S., et al. 2023, *Phys. Dark Univ.*, 41, 101231, doi: [10.1016/j.dark.2023.101231](https://doi.org/10.1016/j.dark.2023.101231)
- Blaineau, T., et al. 2022, *Astron. Astrophys.*, 664, A106, doi: [10.1051/0004-6361/202243430](https://doi.org/10.1051/0004-6361/202243430)
- Boehm, C., Kobakhidze, A., O'hare, C. A. J., Picker, Z. S. C., & Sakellariadou, M. 2021, *JCAP*, 03, 078, doi: [10.1088/1475-7516/2021/03/078](https://doi.org/10.1088/1475-7516/2021/03/078)
- Bonetti, M., & Sesana, A. 2020, *Phys. Rev. D*, 102, 103023, doi: [10.1103/PhysRevD.102.103023](https://doi.org/10.1103/PhysRevD.102.103023)
- Cappellari, M., Neumayer, N., Reunanen, J., et al. 2009, *Mon. Not. Roy. Astron. Soc.*, 394, 660, doi: [10.1111/j.1365-2966.2008.14377.x](https://doi.org/10.1111/j.1365-2966.2008.14377.x)
- Carr, B., Kohri, K., Sendouda, Y., & Yokoyama, J. 2021, *Rept. Prog. Phys.*, 84, 116902, doi: [10.1088/1361-6633/ac1e31](https://doi.org/10.1088/1361-6633/ac1e31)
- Carr, B. J. 1975, *Astrophys. J.*, 201, 1, doi: [10.1086/153853](https://doi.org/10.1086/153853)
- Carr, B. J., & Hawking, S. W. 1974, *Mon. Not. Roy. Astron. Soc.*, 168, 399, doi: [10.1093/mnras/168.2.399](https://doi.org/10.1093/mnras/168.2.399)
- Chen, Z.-C., & Huang, Q.-G. 2018, *Astrophys. J.*, 864, 61, doi: [10.3847/1538-4357/aad6e2](https://doi.org/10.3847/1538-4357/aad6e2)
- Coccia, E. 2024, *PoS, ICRC2023*, 1591, doi: [10.22323/1.444.1591](https://doi.org/10.22323/1.444.1591)
- Colpi, M., et al. 2024. <https://arxiv.org/abs/2402.07571>
- Correa, C. A., Wyithe, J. S. B., Schaye, J., & Duffy, A. R. 2015, *Mon. Not. Roy. Astron. Soc.*, 452, 1217, doi: [10.1093/mnras/stv1363](https://doi.org/10.1093/mnras/stv1363)
- de Blok, W. J. G. 2010, *Adv. Astron.*, 2010, 789293, doi: [10.1155/2010/789293](https://doi.org/10.1155/2010/789293)
- Fakhry, S., Salehnia, Z., Shirmohammadi, A., Ghodsi Yengejeh, M., & Firouzjaee, J. T. 2023, *Astrophys. J.*, 947, 46, doi: [10.3847/1538-4357/acc1dd](https://doi.org/10.3847/1538-4357/acc1dd)
- Feng, W.-X. 2023, PhD thesis, UC, Riverside (main)
- Ferrarese, L., & Merritt, D. 2000, *Astrophys. J. Lett.*, 539, L9, doi: [10.1086/312838](https://doi.org/10.1086/312838)
- Ferrer, F., da Rosa, A. M., & Will, C. M. 2017, *Phys. Rev. D*, 96, 083014, doi: [10.1103/PhysRevD.96.083014](https://doi.org/10.1103/PhysRevD.96.083014)
- Franciolini, G., Baibhav, V., De Luca, V., et al. 2022, *Phys. Rev. D*, 105, 083526, doi: [10.1103/PhysRevD.105.083526](https://doi.org/10.1103/PhysRevD.105.083526)
- Gair, J. R., Barack, L., Creighton, T., et al. 2004, *Class. Quant. Grav.*, 21, S1595, doi: [10.1088/0264-9381/21/20/003](https://doi.org/10.1088/0264-9381/21/20/003)
- Gebhardt, K., et al. 2000, *Astrophys. J. Lett.*, 539, L13, doi: [10.1086/312840](https://doi.org/10.1086/312840)
- Gillessen, S., Eisenhauer, F., Trippe, S., et al. 2009, *Astrophys. J.*, 692, 1075, doi: [10.1088/0004-637X/692/2/1075](https://doi.org/10.1088/0004-637X/692/2/1075)
- Gnedin, O. Y., & Primack, J. R. 2004, *Phys. Rev. Lett.*, 93, 061302, doi: [10.1103/PhysRevLett.93.061302](https://doi.org/10.1103/PhysRevLett.93.061302)
- Gondolo, P., & Silk, J. 1999, *Phys. Rev. Lett.*, 83, 1719, doi: [10.1103/PhysRevLett.83.1719](https://doi.org/10.1103/PhysRevLett.83.1719)
- Gong, Y., Luo, J., & Wang, B. 2021, *Nature Astron.*, 5, 881, doi: [10.1038/s41550-021-01480-3](https://doi.org/10.1038/s41550-021-01480-3)
- Gultekin, K., Richstone, D. O., Gebhardt, K., et al. 2009, *Astrophys. J.*, 698, 198, doi: <https://doi.org/10.1088/0004-637X/698/1/198>
- Hopman, C., & Alexander, T. 2005, *Astrophys. J.*, 629, 362, doi: [10.1086/431475](https://doi.org/10.1086/431475)
- . 2006a, *Astrophys. J. Lett.*, 645, L133, doi: [10.1086/506273](https://doi.org/10.1086/506273)
- . 2006b, *Astrophys. J.*, 645, 1152, doi: [10.1086/504400](https://doi.org/10.1086/504400)
- Hütsi, G., Raidal, M., Vaskonen, V., & Veermäe, H. 2021, *JCAP*, 03, 068, doi: [10.1088/1475-7516/2021/03/068](https://doi.org/10.1088/1475-7516/2021/03/068)
- Jangra, P., Kavanagh, B. J., & Diego, J. M. 2023, *JCAP*, 11, 069, doi: [10.1088/1475-7516/2023/11/069](https://doi.org/10.1088/1475-7516/2023/11/069)
- Jedamzik, K. 2020, *JCAP*, 09, 022, doi: [10.1088/1475-7516/2020/09/022](https://doi.org/10.1088/1475-7516/2020/09/022)
- . 2021, *Phys. Rev. Lett.*, 126, 051302, doi: [10.1103/PhysRevLett.126.051302](https://doi.org/10.1103/PhysRevLett.126.051302)
- Kavanagh, B. J. 2019, bradkav/PBHbounds: Release version, Zenodo, doi: [10.5281/ZENODO.3538999](https://doi.org/10.5281/ZENODO.3538999)
- Kawamura, S., et al. 2021, *PTEP*, 2021, 05A105, doi: [10.1093/ptep/ptab019](https://doi.org/10.1093/ptep/ptab019)
- Kormendy, J., & Ho, L. C. 2013, *Ann. Rev. Astron. Astrophys.*, 51, 511, doi: [10.1146/annurev-astro-082708-101811](https://doi.org/10.1146/annurev-astro-082708-101811)
- Lenoci, A. 2023, PhD thesis, U. Hamburg (main), Hamburg U.

- Li, G.-L., Tang, Y., & Wu, Y.-L. 2022, *Sci. China Phys. Mech. Astron.*, 65, 100412, doi: [10.1007/s11433-022-1930-9](https://doi.org/10.1007/s11433-022-1930-9)
- Loudas, N., Pavlidou, V., Casadio, C., & Tassis, K. 2022, *Astron. Astrophys.*, 668, A166, doi: [10.1051/0004-6361/202244978](https://doi.org/10.1051/0004-6361/202244978)
- Ludlow, A. D., Navarro, J. F., Angulo, R. E., et al. 2014, *Mon. Not. Roy. Astron. Soc.*, 441, 378, doi: [10.1093/mnras/stu483](https://doi.org/10.1093/mnras/stu483)
- Mazzolari, G., Bonetti, M., Sesana, A., et al. 2022, *Mon. Not. Roy. Astron. Soc.*, 516, 1959, doi: [10.1093/mnras/stac2255](https://doi.org/10.1093/mnras/stac2255)
- Merritt, D. 2003, in *Carnegie Observatories Centennial Symposium. 1. Coevolution of Black Holes and Galaxies*. <https://arxiv.org/abs/astro-ph/0301257>
- Merritt, D. 2013, *Dynamics and Evolution of Galactic Nuclei* (Princeton University Press)
- Merritt, D., Alexander, T., Mikkola, S., & Will, C. M. 2011, *Phys. Rev. D*, 84, 044024, doi: [10.1103/PhysRevD.84.044024](https://doi.org/10.1103/PhysRevD.84.044024)
- Merritt, D., Milosavljevic, M., Verde, L., & Jimenez, R. 2002, *Phys. Rev. Lett.*, 88, 191301, doi: [10.1103/PhysRevLett.88.191301](https://doi.org/10.1103/PhysRevLett.88.191301)
- Meszáros, P. 1974, *Astron. Astrophys.*, 37, 225
- Mouri, H., & Taniguchi, Y. 2002, *Astrophys. J. Lett.*, 566, L17, doi: [10.1086/339472](https://doi.org/10.1086/339472)
- Mukherjee, D., Zhou, Y., Chen, N., Di Carlo, U. N., & Di Matteo, T. 2024. <https://arxiv.org/abs/2409.19095>
- Naoz, S., & Haiman, Z. 2023, *Astrophys. J. Lett.*, 955, L27, doi: [10.3847/2041-8213/acf8c9](https://doi.org/10.3847/2041-8213/acf8c9)
- Naoz, S., Rose, S. C., Michaely, E., et al. 2022, *Astrophys. J. Lett.*, 927, L18, doi: [10.3847/2041-8213/ac574b](https://doi.org/10.3847/2041-8213/ac574b)
- Navarro, J. F., Frenk, C. S., & White, S. D. M. 1996, *Astrophys. J.*, 462, 563, doi: [10.1086/177173](https://doi.org/10.1086/177173)
- Nishikawa, H., Kovetz, E. D., Kamionkowski, M., & Silk, J. 2019, *Phys. Rev. D*, 99, 043533, doi: [10.1103/PhysRevD.99.043533](https://doi.org/10.1103/PhysRevD.99.043533)
- O’Leary, R. M., Kocsis, B., & Loeb, A. 2009, *Mon. Not. Roy. Astron. Soc.*, 395, 2127, doi: [10.1111/j.1365-2966.2009.14653.x](https://doi.org/10.1111/j.1365-2966.2009.14653.x)
- Ostriker, J. P. 2000, *Phys. Rev. Lett.*, 84, 5258, doi: [10.1103/PhysRevLett.84.5258](https://doi.org/10.1103/PhysRevLett.84.5258)
- Prada, F., Klypin, A. A., Cuesta, A. J., Betancort-Rijo, J. E., & Primack, J. 2011, *Mon. Not. Roy. Astron. Soc.*, 423, 3018, doi: <https://doi.org/10.1111/j.1365-2966.2012.21007.x>
- Preto, M., & Amaro-Seoane, P. 2010, *Astrophys. J. Lett.*, 708, L42, doi: [10.1088/2041-8205/708/1/L42](https://doi.org/10.1088/2041-8205/708/1/L42)
- Quinlan, G. D., & Shapiro, S. L. 1989, *Astrophys. J.*, 343, 725, doi: [10.1086/167745](https://doi.org/10.1086/167745)
- Raidal, M., Spethmann, C., Vaskonen, V., & Veermäe, H. 2019, *JCAP*, 02, 018, doi: [10.1088/1475-7516/2019/02/018](https://doi.org/10.1088/1475-7516/2019/02/018)
- Raidal, M., Vaskonen, V., & Veermäe, H. 2017, *JCAP*, 09, 037, doi: [10.1088/1475-7516/2017/09/037](https://doi.org/10.1088/1475-7516/2017/09/037)
- Reardon, D. J., et al. 2023, *Astrophys. J. Lett.*, 951, L6, doi: [10.3847/2041-8213/acdd02](https://doi.org/10.3847/2041-8213/acdd02)
- Reitze, D., et al. 2019, *Bull. Am. Astron. Soc.*, 51, 035. <https://arxiv.org/abs/1907.04833>
- Rom, B., Linial, I., Kaur, K., & Sari, R. 2024. <https://arxiv.org/abs/2406.19443>
- Sadeghian, L., Ferrer, F., & Will, C. M. 2013, *Phys. Rev. D*, 88, 063522, doi: [10.1103/PhysRevD.88.063522](https://doi.org/10.1103/PhysRevD.88.063522)
- Sasaki, M., Suyama, T., Tanaka, T., & Yokoyama, S. 2016, *Phys. Rev. Lett.*, 117, 061101, doi: [10.1103/PhysRevLett.117.061101](https://doi.org/10.1103/PhysRevLett.117.061101)
- Shankar, F., Salucci, P., Granato, G. L., De Zotti, G., & Danese, L. 2004, *Mon. Not. Roy. Astron. Soc.*, 354, 1020, doi: [10.1111/j.1365-2966.2004.08261.x](https://doi.org/10.1111/j.1365-2966.2004.08261.x)
- Shapiro, S. L., & Paschalidis, V. 2014, *Phys. Rev. D*, 89, 023506, doi: [10.1103/PhysRevD.89.023506](https://doi.org/10.1103/PhysRevD.89.023506)
- Shi, Y., Zhang, Z.-Y., Wang, J., et al. 2021, *Astrophys. J.*, 909, 20, doi: [10.3847/1538-4357/abd777](https://doi.org/10.3847/1538-4357/abd777)
- Tisserand, P., et al. 2007, *Astron. Astrophys.*, 469, 387, doi: [10.1051/0004-6361:20066017](https://doi.org/10.1051/0004-6361:20066017)
- Tremaine, S., et al. 2002, *Astrophys. J.*, 574, 740, doi: [10.1086/341002](https://doi.org/10.1086/341002)
- Turner, M. 1977, *Astrophys. J.*, 216, 610, doi: [10.1086/155501](https://doi.org/10.1086/155501)
- Ullio, P., Zhao, H., & Kamionkowski, M. 2001, *Phys. Rev. D*, 64, 043504, doi: [10.1103/PhysRevD.64.043504](https://doi.org/10.1103/PhysRevD.64.043504)
- Vika, M., Driver, S. P., Graham, A. W., & Liske, J. 2009, *Mon. Not. Roy. Astron. Soc.*, 400, 1451, doi: <https://doi.org/10.1111/j.1365-2966.2009.15544.x>
- Wang, Y.-F., Huang, Q.-G., Li, T. G. F., & Liao, S. 2020, *Phys. Rev. D*, 101, 063019, doi: [10.1103/PhysRevD.101.063019](https://doi.org/10.1103/PhysRevD.101.063019)
- Wyzykowski, L., Skowron, J., Kozłowski, S., et al. 2011, *Mon. Not. Roy. Astron. Soc.*, 416, 2949, doi: [10.1111/j.1365-2966.2011.19243.x](https://doi.org/10.1111/j.1365-2966.2011.19243.x)
- Xu, H., et al. 2023, *Res. Astron. Astrophys.*, 23, 075024, doi: [10.1088/1674-4527/acdfa5](https://doi.org/10.1088/1674-4527/acdfa5)
- Zahid, H. J., Sohn, J., & Geller, M. J. 2018, *Astrophys. J.*, 859, 96, doi: [10.3847/1538-4357/aabe31](https://doi.org/10.3847/1538-4357/aabe31)
- Zhou, Y., Mukherjee, D., Chen, N., et al. 2024. <https://arxiv.org/abs/2409.19914>